

1 Investigation of hydrological time series using copulas for detecting

2 catchment characteristics and anthropogenic impacts

3 Takayuki Sugimoto¹, András Bárdossy^{1,2} and Geoffrey G. S. Pegram²,Johannes Cullmann³

4
5 1 Institute for Modelling Hydraulic and Environmental Systems, University of Stuttgart, Stuttgart, Germany

6 2 Civil Engineering Program, University of KwaZulu-Natal, Durban, South Africa

7 3 Federal Institute of Hydrology, Koblenz, Germany

8 **Abstract.** Global climate change can have impacts on characteristics of rainfall-runoff
9 events and subsequently on the hydrological regime. Meanwhile, the catchment itself
10 changes due to anthropogenic influences. [However, it is not easy to prove the causality](#)
11 [between them in general.](#) In this context, it can be meaningful to detect the temporal
12 changes of catchments independent from climate change by investigating existing long
13 term discharge records. For this purpose, a new stochastic system based on copulas for
14 time series analysis is introduced. While widely used time series models are based on
15 linear combinations of correlations assuming a Gaussian behavior of variables, a statistical
16 tool like copula has the advantage to scrutinize the dependence structure of the data in the
17 uniform domain independent of the marginal.

18 Two measures in the copula domain are introduced herein:

19 1. Copula asymmetry is defined for copulas and calculated for discharges; this measure
20 describes the non symmetric property of the dependence structure and differs from one
21 catchment to another due to the intrinsic nature of both runoff and catchment.

22 2. Copula distance is defined as Cramér-von Mises type distance calculated between
23 two copula densities of different time scales. This measure describes the variability and
24 interdependency of dependence structures similar to variance and covariance, which can
25 assist in identifying the catchment changes.

26 These measures are calculated for 100 years of daily discharges for the Rhine rivers.
27 Comparing the results of copula asymmetry and copula distance between an API
28 ([Antecedent Precipitation Index](#)) and simulated discharge time series by a hydrological
29 model we can show the interesting signals of systematic modifications along the Rhine
30 rivers in the last 30 years.

31 **Keywords :** Catchment discharge characteristics, Copula stochastic analysis, API, Model
32 uncertainty

33 1. Introduction

34 In order to understand the water cycle behavior of a region, it is important to determine its characteristics,
35 but this is difficult to achieve due to the diversity of the system response at different time and space scales.
36 In particular, temporal variability makes parameter estimation difficult and the assessment of model
37 uncertainty essential. As a part of the endeavor to grasp the hydrological system, the objective of this
38 research, assessing the anthropogenic impacts on the catchment characteristic independent of the climate
39 change is therefore important, yet hard to accomplish.

40 The first possible approach is to statistically test the existence or change of trend in hydrological time
41 series which can be related to climate changes or anthropogenic impacts. Mann-Kendall's Test was
42 performed to confirm the existence of a trend in the annual discharge, precipitation and sediment loads, [then](#)
43 ~~and discussed~~ the human intervention and climate impacts based on the available information of the catchments
44 [were discussed](#) (Wu et al., 2012). Pettitt's Method (Pettitt, 1979) can be used to detect the time point of trend
45 alternation and analyze the impacts based on a double mass curve (Gao et al., 2012) or a hydrological model
46 (Karlsson et al., 2014). These non-parametric methods for detecting the signal seem, however, not capable
47 enough of explaining when and how much the system had changed, thus making it still difficult to relate the
48 change ~~with~~ [to](#) human activities.

49 On the other hand, runoff events are initiated by precipitation then modified by the state and physical
50 features of the catchment. This implies that the integrated information of catchment status might be
51 retrieved by analyzing the discharge time series itself. Focusing on this property, the attempts can be made
52 for capturing the temporal dependence structure of runoff by time series models. The classical time series
53 model, autoregressive integrated moving average (ARIMA), is designed to describe a stationary stochastic
54 process based on the temporal correlation structure of Gaussian random variables (Box and Jenkins, 1976).
55 However, the stationarity of the data is not guaranteed in reality, thus a number of alternative approaches
56 have been suggested. While the application of Fourier Analysis is basically for stationary process, the
57 analysis using empirical mode decomposition (Huang et al., 1998) is overcomes the restriction of
58 stationarity a method designed to overcome the drawbacks of Fourier analysis by allowing the frequency
59 and local variance of a time series to vary within a component and to separate the signals adaptively by
60 scale. Autoregressive Conditional Heteroskedasticity (ARCH) models loose the assumption of stationarity
61 to a certain extent so that variance is not constant, however models the variance in a similar way to
62 ARIMA. Although the inventions and efforts to overcome the limitation of stationarity are made, it seems
63 still inadequate to model dynamic changes of hydrological processes with these time series models.

64 Alternatively there is a statistical concept, copulas, which has advantages to model the multivariate
65 dependence independently from marginals and recently adopted in the field of hydrology. A Copula (Sklar,
66 1959) is a multivariate probability distribution designed to flexibly model dependence structure in the
67 uniform (quantile) domain. The use of copulas in hydrology can be found for the assessment of extreme
68 events by considering flooding as a joint behavior of peak and volume (De Michele and Salvadori, 2003).
69 Copulas have been applied to describe the spatio-temporal uncertainty of precipitation (Bárdossy and
70 Pegram, 2009) or the inhomogeneity of groundwater parameters (Bárdossy and Li, 2008). Asymmetry of
71 dependence in a time series can be tested in the framework of a finite state Markov chain's transition
72 probability matrix (Sharifdoost et al., 2009). Dissimilarity measures can be defined by means of a copula
73 modelling the correlation structure of pairs of discharge time series in order to identify the similarity of

catchments with the purpose of transferring catchment properties from one to the other (Samaniego et al., 2010). We aim at utilizing copulas as an alternative to classical time series models and an efficient tool for time series analysis to overcome these hydrological challenges.

The main interest of this study is to precisely assess the human intervention and climate change impacts on hydrological regime for the strategy of future development in the region. For achieving this goal, 7 daily discharge gauging stations in South-West Germany (Figure 1), which have 100 years daily discharge records, were chosen and extensively analyzed. The gauging stations Andernach, Kaub, Worms and Maxau are located in the main stream of the Rhine, while Kalkofen, Cochem and Plochingen are located on tributaries. For further analysis, daily precipitation and temperature records in the Baden-Württemberg state of Germany for the last 50 years were obtained from the German Weather Service. Also, 77 discharge records obtained from the Global Runoff Data Centre in Germany were utilized.

What follows is the new aspects introduced in this study: (1) The catchment characteristic is defined based on copulas and estimated from discharge data. Also the changes of catchment characteristic are investigated by tracing the temporal change of these statistics. (2) A method to model systematic changes of dependence structure with the help of copulas is suggested, then its variability and interrelationship of the time series are examined. (3) Anthropogenic impacts are assessed by the discharge - precipitation relation using API and hydrological model with copula based measures.

This article is divided into five sections. After the introduction, the basic methodology for applying copulas to discharge time series is introduced in the second section. Thirdly, the measures of asymmetry in copulas are defined and estimated for the discharges of the river Rhine and other catchments. The determination of the temporal change of the asymmetry of the copulas is treated in the third section as well. In the fourth section two topics are treated: (i) the analysis based on copula distances for the observed discharges and (ii) the comparison of observed discharge with API (Antecedent Precipitation Index) time series and simulated discharge time series with a hydrological model. The conclusion is given in the fifth section.

99 2. Methodology

100 In this section, the application of copula to time series is articulated after a brief introduction of copulas.
101 The very basics about copulas are presented here and further information can be obtained from (Joe, 1997)
102 or (Nelsen, 2006).

103 2.1 Basic Methodology

104 In probability theory and statistics, a copula is a multivariate probability distribution for which the
105 marginal probability distribution of each variable is uniform.

106
$$C : [0,1]^n \rightarrow [0,1] \quad (1)$$

107
$$C(\mathbf{u}^{(i)}) = u_i \quad \text{if } \mathbf{u}^{(i)} = (1, \dots, 1, u_i, 1, \dots, 1) \quad (2)$$

108 Any multivariate distribution can be described by a copula and its marginal distributions as was proven by
109 Sklar's theorem (Sklar, 1959):

110
$$F(\mathbf{x}) = C(F_{x_1}(x_1), \dots, F_{x_n}(x_n)) \quad (3)$$

111 where $F_{x_i}(x_i)$ represents the i-th marginal distribution of a multivariate random variable \mathbf{X} . The copula
112 density can be derived by taking partial derivatives of the copula:

113
$$c(u_1, \dots, u_n) = \frac{\partial^n C(u_1, \dots, u_n)}{\partial u_1 \dots \partial u_n} \quad (4)$$

114 The advantage of using copulas is that the marginal is detached from the multivariate distribution and
115 the dependence structure can be examined in the uniform compact domain for different types of data.

116 2.2 Basic Hypothesis of Temporal Copulas

117 For the application of copulas to time series analysis, a stochastic system should be presumed to be
118 similar to the case of spatial copulas (Bárdossy and Li, 2008): the random variable at time t is described as
119 $Z(t)$ and in general there may exist non-Gaussian dependency among the elements of $Z(t)$. Then

Feldfunktion geändert

Feldfunktion geändert

Feldfunktion geändert

Feldfunktion geändert

stationarity is defined for each subset of times $t_1, \dots, t_n \subset N$ and time lag k such that $\{t_1 + k, \dots, t_n + k\} \subset N$ and for each set of possible values z_1, \dots, z_n :

$$\begin{aligned} P(Z(t_1) < z_1, \dots, Z(t_n) < z_n) = \\ P(Z(t_1 + k) < z_1, \dots, Z(t_n + k) < z_n) \end{aligned} \quad (5)$$

Feldfunktion geändert

For the given random function $Z(t)$, a set $S(k)$ containing pairs of ranked values is defined as a function of time lag k as follows:

$$S(k) = \left\{ \left(F_z(z(t)), F_z(z(t+k)) \right) \right\} \quad (6)$$

Feldfunktion geändert

Thus, a 2-dimensional autocopula for stochastic time series is a function of time lag k for the set $S(k)$

similar to the case of aspatial copula (Bárdossy and Li, 2008):

$$C_t(k, u_1, u_2) = P[F_z(Z(t)) < u_1, F_z(Z(t+k)) < u_2] \quad (7)$$

Feldfunktion geändert

where $(u_1, u_2) \in S(k)$. Thus, a 2-dimensional empirical copula density can be constructed based on

conditional empirical frequencies on a regular $g \times g$ grid and kernel density smoothing (Bárdossy, 2006):

$$\begin{aligned} c^* \left(\frac{2i-1}{2g}, \frac{2j-1}{2g} \right) = \frac{g^2}{|S(k)|} \\ \cdot \left| \left\{ (u_1, u_2) \in S(k); \frac{i-1}{g} < u_1 < \frac{i}{g} \text{ and } \frac{j-1}{g} < u_2 < \frac{j}{g} \right\} \right| \end{aligned} \quad (8)$$

Feldfunktion geändert

where $|S(k)|$ denotes the cardinality (the number of elements in a set) of set $S(k)$.

3. Copula Asymmetry in Discharge Time Series

High and low values might have different dependences in general. Measuring the asymmetry of copulas could reveal substantial aspects of time series data, which are not illuminated in the Gaussian approach. Statistics defined on copula shape and calculated from observed discharge time series we believe to be a

new idea. Asymmetry functions are defined on 2-dimensional copulas as a function of time lag k (Li, 2010):

Asymmetry 1 is defined as:

$$A_1(k) = E[(U_t - 0.5)(U_{t+k} - 0.5)((U_t - 0.5) + (U_{t+k} - 0.5))] \\ = \int_0^1 \int_0^1 (u - 0.5)(v - 0.5)(u + v - 1)c(u, v) du dv$$

$$\underline{A_1(k) = E[(U_t - 0.5)(U_{t+k} - 0.5)((U_t - 0.5) + (U_{t+k} - 0.5))]} \quad (9)$$

Feldfunktion geändert

Asymmetry 2 is defined as:

$$\underline{A_2(k) = E[(U_t - 0.5)(U_{t+k} - 0.5)((U_t - 0.5) - (U_{t+k} - 0.5))]} \quad (10)$$

Feldfunktion geändert

$$A_2(k) = E[-(U_t - 0.5)(U_{t+k} - 0.5)((U_t - 0.5) - (U_{t+k} - 0.5))] \\ = \int_0^1 \int_0^1 -(u - 0.5)(v - 0.5)(u - v)c(u, v) du dv$$

where $u_t = F_Z(z(t))$, $u_{t+k} = F_Z(z(t+k))$. Figure 2 shows an idealization of the two asymmetries between a pair of variables $U(t)$ and $U(t+k)$, showing that the tails of the distributions have a large impact on each type of asymmetry. The measure of asymmetry A_1 compares the dependency between low and high values and A_2 quantifies how much it is not symmetric. For example, in a 2-dimensional copula, $A_1(k)$ is positive if the probability density is higher in the upper right corner than in the lower left corner.

On the contrary the other hand, $A_1(k)$ is negative if the probability density is higher in the lower left corner than in the upper right. $A_2(k)$ is the asymmetry for the other diagonal of a 2-dimensional copula.

Figure 3 shows the scatterplot of ranked values of a discharge time series with time lag $k = 1$ as a sample of an empirical autocopula and its connection with storm water hydrographs relation. Demonstrating (i) the dependence structure is not symmetric especially for $A_2(k)$, this figure illustrates (ii) where each pairs of values on hydrograph can be plotted on empirical copula.

For example, sharp rise up of stream flow, which can be characterized as combination of low to high values in empirical copula, is plotted on upper left corner which contributes to the smaller value of asymmetry2 according to the Eq (10)(10)(10). This intrigues the notion that asymmetry might be used for advanced modeling of hydrological time series.

Feldfunktion geändert

Figure 3 shows the scatterplot of ranked values of a discharge time series with time lag $k=1$ as a sample of an empirical autocopula, demonstrating the structure is not symmetric especially for $A_2(k)$.

3.1 Asymmetry and catchment characteristics

Asymmetries can be considered as statistics calculated from the observed discharge time series and leads to have an important assumption: ‘assymetry2 is related to catchment characteristics’. This idea will be exclusively intensively discussed and demonstrated in this section. Figure 5 (upper left) shows part of the hydrographs of 7 gauging stations in southwest Germany.

First, an important ~~and obvious~~ natural property of discharge seen in this figure is that the duration of high flow and low flow periods is not symmetric: Flood events, which are initiated by rainfall or snowmelt, do not continue for a long time because the duration of runoff to rivers is comparatively short. On the other hand, discharge keeps decreasing and stays low for no rain periods. This means that, if two consecutive values in a time series are chosen for small time lag k , these two values are likely to be less correlated for high values but more correlated for low values, which leads to negative value of $A_1(k)$. This asymmetry can be related to the intrinsic temporal distribution of precipitation.

Second, the increase and decrease of discharge is not symmetric: Soon after the rainfall, the river flow rises sharply. Once the rain stops and peak discharge is observed, then the water level starts to decrease, typically more slowly on the recession than the rising limb of the hydrograph, which leads to negative values of $A_2(k)$ for small time lags k . This asymmetry can be related to the characteristics of the runoff and catchment.

The change of $A_2(k)$ with time lag k [days] is now discussed. The point is that these statistics for small time lags k can be more related to the catchment and rainfall characteristics of the region, while asymmetry for larger time lags k can capture the inter-seasonal characteristic of the climate in the region.

Feldfunktion geändert

In order to reduce such seasonal impacts in hydrological time series deseasonalization measure can be applied, for example, especially for daily stream flow (Grimaldi, 2004). Following this method, all the time series are normalized in this study.

~~In order to reduce this seasonal impact, normalization was adopted for the time series similar to z score in the following way. First, the annual cycle of the mean μ_i on the i-th calendar day is calculated as expectation of random variable X_i . Then, the annual cycle of the mean μ_i^* is calculated as smoothed version of μ_i by linearly weighting the neighboring values along i and summing up them. The annual cycle of standard deviation σ_i^* can be obtained in the same way. Then the normalized time series are defined by dividing the original time series $Z(t)$ by σ_i^* after subtracting μ_i^* as follow~~

$$Z_{norm}(t) = \frac{Z(t) - \mu_t^*}{\sigma_t^*} \quad (11)$$

~~and smoothed by linear weighting~~

$$\begin{aligned} \mu_{t|365} &= E[X_{t|365}] \\ \mu_{t|365}^* &= \frac{1}{2N} \sum_{i=0}^{N/2} \left(\frac{1}{2} - \frac{i}{N} \right) (\mu_{t+i|365} + \mu_{t-i|365}) \end{aligned} \quad (11)$$

~~where $t|365$ is $t \pmod{365}$ and represents calendar day at time t [day]. X_i denotes the random variable of discharge, μ_i denotes mean and μ_i^* denotes mean after smoothing on calendar day i respectively. After subtraction of the annual mean from the original time series $Z(t)$, the annual cycle of standard deviation is defined.~~

$$\begin{aligned} \sigma_{t|365} &= E \left[\sqrt{(X_{t|365} - \mu_{t|365})^2} \right] \\ \sigma_{t|365}^* &= \frac{1}{2N} \sum_{i=0}^{N/2} \left(\frac{1}{2} - \frac{i}{N} \right) (\sigma_{t+i|365} + \sigma_{t-i|365}) \end{aligned} \quad (12)$$

Figure 4 shows the annual cycles after smoothing described by equations (11) and (12). By subtracting the annual mean cycle and dividing by annual standard deviation cycle, the normalized time series is defined.

Formatiert: Tiefergestellt durch 15 Pt.

Feldfunktion geändert

Formatiert: Text

Formatiert: Text

$$Z_{norm}(t) = \frac{Z(t) - \mu_{t|365}^*}{\sqrt{\sigma_{t|365}^*}} \quad (13)$$

Figure 5 (upper right) shows part of normalized discharge time series from the 7 gauging stations. It should be noted that the process still appears to be non-Gaussian after this transformation and the seasonality for small time lags k might not be fully eliminated. Figure 5 (bottom left and bottom right) shows the variation of asymmetry functions for 7 discharge time series corresponding to time lag k similar to the correlograms in addition to the confidence interval of Gaussian process.

The confidence intervals in the figures are gained by calculating $A_2(k)$ for 100 realizations of stationary Gaussian process which are fitted to the observed discharge of Andernach. The result shows that the process is clearly different from Gaussian and the influence of asymmetry is significantly large.

It can be seen that the variation of $A_2(k)$ of discharge without normalization (Figure 5 bottom left) has a larger impact of seasonality for bigger k ($k > 40$), while its impacts are mitigated after the normalization (Figure 5 bottom right). Furthermore, as a consequence of normalization, a sharp drop down of $A_2(k)$ for small time lags k emerged which might be regarded as a catchment indicator. Therefore, the selected/critical properties for small time lags k is formulated by (i) taking the minimum value of $A_2(k)$ for the time lag $k < 50$ and (ii) the lag k at the minimum of asymmetry2:

$$A_{2,\min} = \min_{k < 50} A_2(k) \quad (12)$$

$$L_{2,\min} = \min_{0 < k < 50} \{k; A_2(k) = A_{2,\min}\} \quad (13)$$

The question is whether they are really related to catchment characteristics. Now, these statistics estimated for 77 discharge data recorded at the gauging stations in Germany are compared with the catchment area as one of the simplest possible indicators of the catchment as shown in Figure 6: $A_{2,\min}$ -

area (Figure 6 top) and shows a more clear linear relation than $L_{2,\min}$ - area (Figure 6 middle) are both showing linear relationship to the log-scaled x-axis of catchment area with positive correlation. There

seems also the linear relation between $A_{2,\min}$ and $L_{2,\min}$ as a consequence of above relationships. for the smaller catchments are big for both cases. The correlation between $A_{2,\min}$ and $L_{2,\min}$ (Figure 6 bottom) is slightly positive.

Feldfunktion geändert

This demonstrates that the information extracted from discharge is related to the basic information of its catchment to a certain extent. Since the principal objective is to assess anthropogenic impacts, the idea introduced now is to use this measure for evaluating the catchment change by calculating chronological changes of $A_{2,\min}$.

3.2 Time Series Analysis with Asymmetry

Temporal change of asymmetry $A_2(k, t)$ is defined on the set representing a moving time window of size w .

$$S^*(k, t) = \left\{ (F_Z(z(a))), (F_Z(z(a+k))); t - \frac{w}{2} < a < t + \frac{w}{2} \right\} \quad (14)$$

Feldfunktion geändert

$$A_2(k, t) = E[-(U_t - 0.5)(U_{t+k} - 0.5)((U_t - 0.5) - (U_{t+k} - 0.5))] \\ = \int_0^1 \int_0^1 -(u_t - 0.5)(u_{t+k} - 0.5)(u_t - u_{t+k})c(u_t, u_{t+k})du_t du_{t+k}$$

(15)

Feldfunktion geändert

where $u_t \in U_t, u_{t+k} \in U_{t+k}, (u_t, u_{t+k}) \in S^*(k, t)$. Then the minimum of asymmetry² and lag k at the minimum of asymmetry² at time t are given by

$$A_{2,\min}(t) = \min_{k < 30} A_2(k, t) \quad (16)$$

Feldfunktion geändert

$$L_{2,\min}(t) = \min_{0 < k < 30} \{k; A_2(k, t) = A_{2,\min}(t)\} \quad (17)$$

Feldfunktion geändert

Figure 7 shows the temporal changes of $A_{2,\min}(t)$ with window size $w = 3000$ [days] for 7 gauging stations in southwest Germany in addition to the confidence interval calculated for 100 times independently generated Gaussian process.

244 The comparison of $A_{2,\min}(t)$ from observed discharges with $A_{2,\min}(t)$ from a Gaussian process exhibits
 245 (i) the influence of asymmetry in discharge is significantly large as it was seen in Figure 5. (ii) The
 246 fluctuations of $A_{2,\min}(t)$ of 7 observed discharge time series appear to be bigger than the one calculated for
 247 a realization of a Gaussian process. (iii) $A_{2,\min}(t)$ of these 7 discharge records shows a similar trend: there
 248 are big drop-downs around 1945 and after 1980 for all the discharges.

249 However, it cannot be ascertained whether this is caused by the simultaneous change of the catchments,
 250 the long term meteorological behavior in the region or just randomness in the stationary process. To
 251 overcome this, temporal behavior of discharge and temperature were first checked by calculating the mean,
 252 the standard deviation and the minimum at time t defined by

$$\begin{aligned}
 Mean(t) &= \frac{1}{w} \int_{t-w/2}^{t+w/2} z(a) da \\
 Std(t) &= \sqrt{Var(t)} = \frac{1}{w} \left(\int_{t-w/2}^{t+w/2} (z(a) - E[Z(t)])^2 da \right)^{\frac{1}{2}} \\
 Min(t) &= \min \left\{ Z(a); t - \frac{w}{2} < a < t + \frac{w}{2} \right\}
 \end{aligned} \tag{18}$$

254 where w is the size of time window. Figure 8 shows moving average and moving standard deviation of
 255 discharge records with windows size $w = 3000$ [days], but it is hard to say whether the behavior around
 256 1945 and after 1980 is unusual. Figure 9 shows mean and minimum of temperature in the time window
 257 with size 365 [days] which correspond to annual mean and minimum. Roughly speaking, there are certain
 258 cold periods around 1940, 1955 and 1985, which might influence the snow accumulation and melting in
 259 the region, but the relation with asymmetry2 is rather obscure.

260 What seems to be a useful outcome from the above exploratory analysis is that (i) the behavior of
 261 asymmetry2 is different from catchment to catchment showing a statistical relation with the catchment area
 262 and (ii) temporal behaviors of asymmetry2 of 7 discharges time series are dependent on each other, which
 263 implies the existence of a background mechanism common to the region.

264 4. Analysis of hydrological time series with Copula Distance

As an alternative to copula asymmetry, which emphasizes the behavior on the corner of copulas, copula distance is here suggested so that the characteristic behavior can be captured in the entire domain of the copula. Calculating this for each time step for different time series and comparing them hopefully exhibits the changes of dependence structure and therefore the catchment change.

4.1 Introduction of Copula Distance

The basic idea behind the copula distance is to apply the Cramér-von Mises type distance

$$D = \int_0^1 \int_0^1 (C^*(u_1, u_2) - C(u_1, u_2))^2 du_1 du_2 \quad (19)$$

, which by design measures the goodness of fit between two distribution functions, to two copulas. This type of distance was tested to measure the difference between empirical and theoretical copula in the bootstrap framework for the evaluation of spatial dependence of ground water quality (Bárdossy, 2006). For the analysis of time series data, it still needs to be carefully thought out how (and which) copulas should be chosen.

4.1.1 Introduction of Copula Distance to single time series

In order to apply the concept of copula distance to time series, the adoption of two copulas in different time scales is considered. An empirical copula can be obtained from an entire time series which contains the averaged information of all the time points (*global copula*). Another empirical copula can be obtained for a certain window of width w at time step t (*local copula*). In order to make the concept clear, two sets containing pairs of ranked values with different time scales are specified.

$$S_{global}(k) = \{(F_Z(z(t))), (F_Z(z(t+k)))\}; t_1 < t < t_n\} \quad (20)$$

$$S_{local}(k, t) = \{(F_Z(z(a))), (F_Z(z(a+k)))\}; t - \frac{w}{2} < a < t + \frac{w}{2}\} \quad (21)$$

$S_{local}(k, t)$ can be interpreted as a moving time window where the reference time t is set to the middle of the window of size w , while $S_{global}(k)$ represents a set of the entire time series. *Global copula* and *local*

287 *copula* are the empirical autocopula densities defined on these sets based on Equation ~~(8)~~(8), there denoted
 288 by $c_{global}^*(\mathbf{u})$ and $c_{local}^*(\mathbf{u}, t, w)$ respectively for the n-dimensional case. In this analysis, 3000 [days] for the
 289 time window w and a 3-dimensional copula separated with 1 day gap between each variable are employed.
 290 This means

$$291 \quad \mathbf{u} = (u_0, u_1, u_2) \quad (22)$$

292 where $u_0 = F_z(Z(t))$, $u_1 = F_z(Z(t+1))$, $u_2 = F_z(Z(t+2))$, then the deviation of local copula from global
 293 copula is defined by

$$294 \quad \Delta c(\mathbf{u}, t) = c_{local}^*(\mathbf{u}, t) - c_{global}^*(\mathbf{u}) \quad (23)$$

295 For the first approach, the comparison of dependence structures between entire and local time series is
 296 done for detecting unusual dependence structures. To this end, *copula distance type1* is defined by taking
 297 the copula distance between global and local copula at each time step t

$$298 \quad \begin{aligned} D_1(c, t) &= \int_0^1 \dots \int_0^1 (c_{global}^*(\mathbf{u}) - c_{local}^*(\mathbf{u}, t))^2 du_1 \dots du_n \\ &= \int_0^1 \dots \int_0^1 \Delta c(\mathbf{u}, t)^2 du_1 \dots du_n \end{aligned} \quad (24)$$

299 Second, *copula distance type 2* is introduced for indicating the point at which the structure of copulas starts
 300 to change. For this method, the distance between two local copulas is calculated from the 2 time intervals

$$301 \quad D_2(c, t) = \int_0^1 \dots \int_0^1 \left(c_{local}^*\left(\mathbf{u}, t - \frac{w}{2}\right) - c_{local}^*\left(\mathbf{u}, t + \frac{w}{2}\right) \right)^2 du_1 \dots du_n \quad (25)$$

302 Note that reference time is set to the middle of both time windows and shifted for $w/2$ [days] from each
 303 other where the size of the time windows is w . Therefore, there is no overlapping part between the two
 304 time intervals of these two local copulas. For the comparison, the moving variance is introduced as
 305 follows:

$$306 \quad \begin{aligned} E[Z(t)] &= \frac{1}{w} \int_{t-w/2}^{t+w/2} z(a) da \\ Var(t) &= \frac{1}{w} \int_{t-w/2}^{t+w/2} (z(a) - E[Z(t)])^2 da \end{aligned} \quad (26)$$

Feldfunktion geändert

Figure 10 shows the result of $D_1(t)$, $D_2(t)$ and $Var(t)$ in the moving time window for the normalized discharge time series between 1940 to 2000 at 4 gauging stations located in the main stream of the Rhine (Andernach, Maxau) and its two different tributaries (Cochem, Plochingen) in addition to the 90 % confidence intervals calculated for the Gaussian process fitted to the discharge data of Andernach.

First of all, the values of these 2 measures at Cochem and Plochingen are bigger and more fluctuating in general. The reason could be that their catchments and discharges are smaller, thus more sensitive to changes. Second, it can be said that the dependence structure is not homogeneous over the time period, but the local copula clearly deviates from the global copula for certain time periods. For example, the value of $D_1(t)$ is remarkably big around 1947, 1982 and 2000 for all the 4 discharge records (pointed by white arrows). $D_2(t)$ is also big around 1977 for all the data. This signal of $D_2(t)$ implies that a simultaneous change of runoff behavior occurred in this region at 1977, which can be related to the high value of $D_1(t)$ at 1982. $Var(t)$ is also changing, but the direct relation with $D_1(t)$ and $D_2(t)$ is hard to recognize. Also the confidence interval of the Gaussian process is clearly smaller than the observed one. This indicates the copula distances of the stationary process are small while the nature process is non-stationary and its dependence structure is more varying.

For copula distance type1, the global copula can be considered as an average state of the copula, while the local copula can be regarded as a realization of a possible state of a copula at time step t . This concept can be comparable to variance and leads to a new measure, *copula variance*, which is the summation of copula distances between global and local copula over the time.

$$Var_{cop}(c) = \frac{1}{t_n - t_1} \int_{t_1}^{t_n} D_1(c, t) dt \quad (27)$$

Feldfunktion geändert

[Table 1](#) shows the variance and copula variance calculated for the 4 discharge data. The result demonstrates that copula variance of the time series can be higher, even if the conventional variance is lower for example in case of Maxau.

330 4.1.2 Copula Distance for two time series

331 In the previous section, copula variance was defined as a measure of the variability characteristic of the
 332 copula itself. Here, it is examined whether covariance can be defined for two copula densities c_1 and c_2
 333 from two time series as *copula distance type3*, which shows whether the variability characteristic of
 334 copulas is related to each other.

$$335 \quad D_3(c_1, c_2, t) = \int_0^1 \dots \int_0^1 \Delta c_1(\mathbf{u}, t) \Delta c_2(\mathbf{u}, t) du_1 \dots du_n \quad (28)$$

336 where

$$337 \quad \begin{aligned} \Delta c_1(\mathbf{u}, t) &= c_{1,local}^*(\mathbf{u}, t) - c_{1,global}^*(\mathbf{u}) \\ \Delta c_2(\mathbf{u}, t) &= c_{2,local}^*(\mathbf{u}, t) - c_{2,global}^*(\mathbf{u}) \end{aligned} \quad (29)$$

338 By its definition, the value of $D_3(t)$ can be related to $D_1(t)$ because $D_3(t)$ compares the deviation of local
 339 copulas from global copulas in a similar way to $D_1(t)$ in Equation (26). In order to reduce the influence of
 340 $D_1(t)$ on $D_3(t)$, *copula distance type4* is introduced as a normalized measure bounded between -1 and 1
 341 analogous to correlation.

$$342 \quad D_4(c_1, c_2, t) = \frac{D_3(c_1, c_2, t)}{\sqrt{D_1(c_1, t)} \cdot \sqrt{D_1(c_2, t)}} \quad (30)$$

343 where $|D_4(c_1, c_2, t)| \leq 1$. For comparison, covariance and correlation in a moving window are introduced for
 344 two random variables $Z_1(t)$ and $Z_2(t)$ as follows:

$$345 \quad Cov(t) = \int_{t-w/2}^{t+w/2} (z_1(a) - E[Z_1(t)])(z_2(a) - E[Z_2(t)]) da \quad (31)$$

$$346 \quad Cor(t) = \frac{Cov(t)}{\sqrt{Var(Z_1(t))} \cdot \sqrt{Var(Z_2(t))}} \quad (32)$$

347 Figure 11 shows the copula distance between two time series $D_3(t)$ and $D_4(t)$ in addition to the
 348 covariance and correlation in moving time window.

First, it can be said that the behavior of covariance and correlation in a moving window are different from $D_3(t)$ and $D_4(t)$. This implies these two copula based statistics exhibit different properties of the time series from ordinary statistics. Second, $D_3(t)$ shows high values around 1947, 1982 and 2000, which is same to the case of $D_1(t)$ in Figure 10. This indicates that unusual states of copulas in 4 discharge time series can be related to each other. Third, $D_4(t)$ is in general high except for the period around 1970 and 1990. This means, the temporal behavior of dependence structures for these 4 discharges are actually similar except for these periods even if $D_1(t)$ and $D_3(t)$ are small.

Copula covariance and copula correlation can be defined similar to copula variance in order to quantify the overall behavior of two time series.

$$Cov_{cop}(c_1, c_2) = \frac{1}{t_2 - t_1} \int_{t_1}^{t_2} D_3(t) dt \quad (33)$$

$$Cor_{cop}(c_1, c_2) = \frac{Cov_{cop}(c_1, c_2)}{\sqrt{Var_{cop}(c_1)} \cdot \sqrt{Var_{cop}(c_2)}} \quad (34)$$

where $|Cor_{cop}(c_1, c_2)| \leq 1$ and its derivation can be found in appendix A. In [Table 2](#), these copula based statistics are compared with ordinary statistics. For example, Cochem and Plochingen are located remotely in different tributaries, thus covariance and correlation are lower than the others, but copula covariance and copula correlation are not the lowest.

The measures using copula distance are different from the conventional statistics. This behavior can be explained by the fact that the autocopula has more substantial information about temporal dependence structure than the autocorrelation. Using these measures might enable us to take advantage of a different way of seeing the dependence between time series.

What is new in the analysis of this section is that (i) measures based on copula distance show the different properties of time series in comparison to conventional statistics and (ii) there are significant signals of copula distances for certain time periods in common to all the discharge data.

371 4.2 Copula based Stochastic Analysis with API and Hydrological Model

372 The difficulty of analyzing discharge time series in order to detect catchment change is that it is not clear
373 whether the temporal change of stochastic information is caused by catchment change or merely by
374 random behavior of precipitation. To gain an understanding of this process, we attempted to eliminate the
375 influence of precipitation using, first, API (antecedent precipitation index) for comparison with discharge ,
376 second, using a hydrological model with the parameter sets calibrated and fixed for the entire simulation
377 time period.

378 4.2.1 Copula Distance Analysis with API

379 An API (Antecedent Precipitation Index) time series, which is generated from observed precipitation
380 time series and behaves similarly to discharge, is used instead of precipitation.

$$381 \quad API(t+1) = \alpha API(t) + P(t+1) \quad (35)$$

Feldfunktion geändert

382 where $P(t)$ is daily precipitation [mm/day], $API(t)$ is time series of API [mm/day] and $\alpha = 0.85$ was
383 chosen. The assumption for this method is that the API time series has the stochastic information purely
384 originated from the precipitation, while observed discharge is supposed to be influenced by both
385 catchments and precipitations. If the stochastic information derived from these two data sets is the same,
386 this indicates that the stochastic turbulence is originating from precipitation; otherwise the change is from
387 the catchment.

388 For this investigation, precipitation data was carefully chosen for 4 regions (northwest, northeast,
389 southwest and central) of Baden-Württemberg (Germany) so that they have several almost continuous
390 daily records between 1935 and 2005. Figure 12 shows the locations of measuring stations. The
391 precipitation time series were aggregated into one for each region by taking daily average, then 4 API time
392 series was calculated in total by Equation ~~(35)~~(35). Figure 13 shows the result of copula distances
393 $D_1(t), D_2(t)$ and moving average $Var(t)$ for API time series with the 90% confidence intervals of the

394 Gaussian process. Figure 14 shows the result of copula distances $D_3(t), D_4(t)$ and moving covariance and
395 correlation for API time series.

396 What can be recognized first in this Figure 13 is that the magnitudes of $D_1(t)$ and $D_2(t)$ are smaller than
397 the case of discharge. This is considered to happen as a result of aggregation of precipitation time series
398 and adoption of API, but some signals can be still identified: $D_1(t)$ around 1947 and 2000 is high, but not
399 much for 1982. The signal of $D_2(t)$ which was detected around 1977 in Figure 11 does not seem to exist
400 for API. This can be even more clear for $D_3(t)$ in Figure 14 that there is no common change of the
401 dependence structure around 1982 in API time series. This is interesting due to the following implications:
402 (i) the noises of $D_1(t)$ in ~~Figure 13~~ [Figure 13](#) were reduced and signals in common were amplified (ii) the
403 unusual state of copula around 1982 is not caused not by precipitation, but could be caused by the
404 catchment change.

405 For further verification, copula distance type3 and type4 between discharge and API time series were
406 calculated as shown in Figure 15. This result also shows there is no clear relation between API and
407 discharge time series around 1982.

408 **4.2.2 Copula based analysis with a hydrological model**

409 API time series were calculated by spatially aggregating several daily precipitations records in each region
410 of Baden-Württemberg state. In this section, simulated discharges time series are generated by a
411 conceptual hydrological model, HBV (Bergström 1976 ; Bergström, Singh, and others 1995) ,which takes
412 daily precipitations and temperatures records as input and simulates discharges for smaller catchments as
413 more robust sample of discharge to compare with observed discharge in order to check if differences might
414 occur due to the method.

415 Thus the idea behind this methodology is similar to the case of API: A hydrological model with the
416 parameters fixed for the entire time period represents the catchment not influenced by anthropogenic

417 impacts. Then, the discharges simulated by this model should not reflect on the catchment change, while
418 observed discharge is assumed to be influenced by both catchment and precipitation.

419 For the study area, Upper Neckar Catchment was chosen as drawn in Figure 12. One parameter set
420 needed for this model constitutes of 13 parameters which are calibrated based on the Nash–Sutcliffe model
421 efficiency coefficient using the simulated annealing algorithm for the period between 1960 and 2000. Then,
422 30 parameter sets are independently calibrated in total and, subsequently, 30 simulated discharges time
423 series are generated to compare with one observed discharge.

424 Figure 16 shows the result of copula based analysis calculated for single time series
425 $(D_1(t), D_2(t), A_{2,\min}(t))$. It can be seen that $A_{2,\min}(t)$ in Figure 16 (top) that (i) fluctuations of $A_{2,\min}(t)$
426 of observed and simulated discharge are locally identical. This implies that the short term behavior of
427 $A_{2,\min}(t)$ is originated from the temporal behavior of precipitation but (ii) there exists a change of trend
428 around 1976: $A_{2,\min}(t)$ of observed discharge is slightly bigger than simulated before 1976, while
429 $A_{2,\min}(t)$ of observed discharge clearly undershoot the simulated ones of after 1976. This change of trend
430 was also seen in the previous analyses ($D_2(t)$ in Figure 10). Furthermore, $D_1(t)$ in Figure 16 (middle) is
431 high before 1976 which indicates the state of the copula is different from the rest, while the result of
432 simulated discharges does not show such tendency. $D_2(t)$ in Figure 16 (bottom) indicates the change of
433 dependence structure happened around 1970 and 1977. These results using the HBV model indicate the
434 change of the dependence structure detected using copulas around 1976 is not caused by the random
435 behavior of precipitation, but by the behavior of the catchment itself.

436 The fact and the notion obtained in this section is that (i) both results from API and HBV based on
437 copula measures indicate that the catchment changed around 1976 and (ii), by comparing the simulated
438 discharge with observed discharge, the origin of the change of stochastically information can be assessed.

439

440 **Conclusion**

441 In this paper the application of copulas for hydrological time series data is newly explored for the
442 detection of catchment characteristics and their temporal changes.

443 1. A Copula based measure, asymmetry, was defined and newly applied for the identification of
444 catchment characteristics. Indeed, it ~~was is presumed~~^{presented} that asymmetry2 ~~is can be~~ related to the
445 runoff characteristics.

446 2. The relation between the minimum of asymmetry2 and catchment characteristics was tested for 77
447 discharge records. Asymmetry2 has a certain relation especially with bigger catchments and this
448 strengthens the notion that asymmetry2 can be used as a statistic to explain the catchment state.

449 3. Temporal change of asymmetry2 was calculated as an index of the catchment state and demonstrated
450 it keeps changing coincidentally with time. However, it is difficult to explain the causality, at least, by long
451 term behavior of discharge and temperature time series.

452 4. A method based on copula distance was examined for the investigation of temporal behavior of
453 hydrological time series. This measure can detect the time period where dependence structure is unusual
454 and its interdependency. Clear signals were detected that the dependence structure is unusual for a certain
455 time period and the signal was not found by investigating the time series with variance, covariance or
456 correlation.

457 5. API time series were generated for each region in the Baden-Württemberg state and simulated
458 discharge time series were generated using the HBV model for the Upper Neckar Catchment. These are the
459 data not influenced by the catchment change, thus compared with observed discharge to assess the
460 anthropogenic impacts. The results showed that there was a signal detected only in the observed discharge
461 around 1982, but not in the API or simulated time series, which implies the anthropogenic impacts on the
462 catchment. Also it was shown in the results of copula asymmetry that ~~the difference of $A_{2,\min}(t)$ between~~
463 ~~observed and simulated discharge was not constant, but~~ the trend clearly changed around 1976.

464 | The results of copula based analysis of hydrological time series [seem to](#) support the assumption that the
465 | catchment had started to change around 1976 and stayed unusual until 1990. These changes could
466 | correspond to the construction of flood retention basins started around 1982 (Lammersen et al., 2002) and
467 | ecological flooding strategy, which let small floods to happen for the rehabilitation of ecological systems
468 | in the floodplain, introduced in the Upper Rhine since 1989 (Siepe, 2006).

469 | Copulas can be an alternative method to analyze the hydrological time series data by focusing on the
470 | dependence structure, [but further applications and theoretical developments are expected in this frame](#)
471 | [work. The copula based techniques introduced here for estimating catchment change can be related to the](#)
472 | [potential model uncertainty.](#)—Empirical autocopula is a more data driven approach which retains more
473 | information than the copulas estimated with parametric methods, but it is also numerically demanding. The
474 | effective way to analyze time series and build up a time series model based on copula can be further
475 | explored.

476 |

Feldfunktion geändert
Feldfunktion geändert
Feldfunktion geändert

477 |

478 |

479 |

480 Appendix A

481 Suppose that a random variable at time t is denoted as $X(t)$ and $c_X(\mathbf{u}, t)$ is an autocopula obtained from
 482 $X(t)$. Assuming $c_{X,mean}(\mathbf{u})$ as an average state of $c_X(\mathbf{u}, t)$, deviation of copula $\Delta c_X(\mathbf{u}, t)$ at time t is
 483 defined by

$$484 \quad \Delta c_X(\mathbf{u}, t) = c_X(\mathbf{u}, t) - c_{X,mean}(\mathbf{u}) \quad (A1)$$

485 For the empirical case, $c_X(\mathbf{u}, t)$ and $c_{X,mean}(\mathbf{u})$ can be regarded as local copula and global copula
 486 respectively similar to Equation ~~(29)~~(29). Since global and local copula are empirical copula density as
 487 defined in equation ~~(8)~~(8), $\Delta c_X(\mathbf{u}, t)$ can be regarded as a vector of values on finite number of grids:

$$488 \quad \Delta \mathbf{c}_X(t) = (\Delta c_{X,1}(t), \Delta c_{X,2}(t), \dots, \Delta c_{X,i}(t), \dots, \Delta c_{X,N}(t)) \quad (A2)$$

489 where $\Delta c_{X,i}(t)$ denotes the value of copula density at i -th grid and N is the number of grids. From
 490 Cauchy-Schwarz inequality

$$491 \quad \|\Delta \mathbf{c}_X(t)\| \|\Delta \mathbf{c}_Y(t)\| \geq \left| \langle \Delta \mathbf{c}_X(t), \Delta \mathbf{c}_Y(t) \rangle \right|^2 \quad (A3)$$

492 where $\|\Delta \mathbf{c}_X(t)\|$ is norm and $\langle \Delta \mathbf{c}_X(t), \Delta \mathbf{c}_Y(t) \rangle$ is inner product of vector $\Delta \mathbf{c}_X(t)$ and $\Delta \mathbf{c}_Y(t)$. Then

$$493 \quad \begin{aligned} \|\Delta \mathbf{c}_X(t)\| &= \sum_{i=1}^N \Delta c_{X,i}(t)^2 \\ &= \int_0^1 \dots \int_0^1 (\Delta c_X(\mathbf{u}, t))^2 du_1 \dots du_n = D_1(c_X, t) \end{aligned} \quad (A4)$$

$$494 \quad \begin{aligned} &\left| \langle \Delta \mathbf{c}_X(t), \Delta \mathbf{c}_Y(t) \rangle \right|^2 \\ &= \langle \Delta \mathbf{c}_X(t), \Delta \mathbf{c}_Y(t) \rangle = \sum_{i=1}^N \Delta c_{X,i}(t) \cdot \Delta c_{Y,i}(t) \\ &= \int_0^1 \dots \int_0^1 \Delta c_X(\mathbf{u}, t) \Delta c_Y(\mathbf{u}, t) du_1 \dots du_n = D_3(c_X, c_Y, t) \end{aligned} \quad (A5)$$

$$495 \quad \frac{\left| \langle \Delta \mathbf{c}_X(t), \Delta \mathbf{c}_Y(t) \rangle \right|^2}{\|\Delta \mathbf{c}_X(t)\| \|\Delta \mathbf{c}_Y(t)\|} = \frac{D_3(c_X, c_Y, t)^2}{D_1(c_X, t) \cdot D_1(c_Y, t)} = D_4(c_X, c_Y, t)^2 \leq 1 \quad (A6)$$

Therefore $|D_4(c_X, c_Y, t)| \leq 1$ in Equation (30)(39). Above inequality is valid for certain time point t and summing up (A6) for all the time steps t leads to

$$\sum_{t=1}^T (\|\Delta \mathbf{c}_X(t)\| \cdot \|\Delta \mathbf{c}_Y(t)\|) \geq \sum_{t=1}^T |\langle \Delta \mathbf{c}_X(t), \Delta \mathbf{c}_Y(t) \rangle| \quad (\text{A7})$$

where T is the number of time steps. $\|\Delta \mathbf{c}_X(t)\|$ is a norm and can be denoted for simplicity as

$x_t = \|\Delta \mathbf{c}_X(t)\|$. Then

$$\sum_{t=1}^T (\|\Delta \mathbf{c}_X(t)\| \|\Delta \mathbf{c}_Y(t)\|) = \langle \mathbf{x}, \mathbf{y} \rangle \quad (\text{A8})$$

where $\mathbf{x} = (x_1, x_2, \dots, x_T)$, $\mathbf{y} = (y_1, y_2, \dots, y_T)$ for $t = 1 \dots T$. Again from Cauchy-Schwarz inequality

$$|\langle \mathbf{x}, \mathbf{y} \rangle|^2 \leq \|\mathbf{x}\| \|\mathbf{y}\| \quad (\text{A9})$$

where

$$\begin{aligned} \|\mathbf{x}\| \cdot \|\mathbf{y}\| &= \sum_{t=1}^T x_t^2 \cdot \sum_{t=1}^T y_t^2 = \sum_{t=1}^T \|\Delta \mathbf{c}_X(t)\|^2 \cdot \sum_{t=1}^T \|\Delta \mathbf{c}_Y(t)\|^2 \\ &= \sum_{t=1}^T D_1(c_X, t)^2 \cdot \sum_{t=1}^T D_1(c_Y, t)^2 = T^2 \cdot \text{Var}_{cop}(c_X) \cdot \text{Var}_{cop}(c_Y) \end{aligned} \quad (\text{A10})$$

$$\begin{aligned} \langle \mathbf{x}, \mathbf{y} \rangle &= \sum_{t=1}^T (x_t \cdot y_t) = \sum_{t=1}^T (\|\Delta \mathbf{c}_X(t)\| \cdot \|\Delta \mathbf{c}_Y(t)\|) \geq \sum_{t=1}^T |\langle \Delta \mathbf{c}_X(t), \Delta \mathbf{c}_Y(t) \rangle| \\ &= \sum_{t=1}^T D_{3,XY}(t) = T \cdot \text{Cov}_{cop}(c_X, c_Y) \end{aligned} \quad (\text{A11})$$

Then $|\langle \mathbf{x}, \mathbf{y} \rangle|^2 \leq \|\mathbf{x}\| \|\mathbf{y}\|$ indicates

$$\begin{aligned} |\text{Cov}_{cop}(c_X, c_Y)|^2 &\leq \text{Var}_{cop}(c_X) \text{Var}_{cop}(c_Y) \\ |\text{Cor}_{cop}| &= \frac{\text{Cov}_{cop}(c_X, c_Y)}{\sqrt{\text{Var}_{cop}(c_X)} \cdot \sqrt{\text{Var}_{cop}(c_Y)}} \leq 1 \end{aligned} \quad (\text{A12})$$

Feldfunktion geändert

Feldfunktion geändert

Feldfunktion geändert

Feldfunktion geändert

Feldfunktion geändert

Feldfunktion geändert

511 **Acknowledgment**

512 Fundamental research of this paper was initiated by the BfG (German Federal Institute of Hydrology)
513 with financial support. Special thanks are given to the Global Runoff Data Centre (GRDC) in Germany
514 for offering the discharge data and the German Meteorological Service (DWD) for precipitation and
515 temperature data. [All the authors deeply appreciate all the reviewers for the efforts for examining and](#)
516 [inspecting this work](#).

Formatiert: Nicht unterstrichen

517 **References**

- 518 Bárdossy, a., Pegram, G., 2009. Copula based multisite model for daily precipitation simulation. Hydrol.
519 Earth Syst. Sci. Discuss. 6, 4485–4534. doi:10.5194/hessd-6-4485-2009
- 520 Bárdossy, A., 2006. Copula-based geostatistical models for groundwater quality parameters. Water Resour.
521 Res. 42, W11416. doi:10.1029/2005WR004754
- 522 Bárdossy, A., Li, J., 2008. Geostatistical interpolation using copulas. Water Resour. Res. 44, W07412.
523 doi:10.1029/2007WR006115
- 524 Bergström, S., 1976. Development and application of a conceptual runoff model for Scandinavian
525 catchments, Bulletin Series A, A]: [Bulletin series. Department of Water Resources Engineering, Lund
526 Institute of Technology, University of Lund.
- 527 Bergstrom, S., 1995. The HBV Model. Singh, V.P. (Ed.), Comput. Model. Watershed Hydrol. 443–476.
- 528 Box, G.E.P., Jenkins, G.M., 1976. Time series analysis: forecasting and control, revised ed. Holden-Day,
529 San Francisco, USA.
- 530 [Brahimi, B., Chebana, F., Necir, A., 2014. Copula representation of bivariate L-moments: a new](#)
531 [estimation method for multiparameter two-dimensional copula models. Statistics \(Ber\). 1–25.](#)
- 532 De Michele, C., Salvadori, G., 2003. A Generalized Pareto intensity-duration model of storm rainfall
533 exploiting 2-Copulas. J. Geophys. Res. Atmos. 108, 4067. doi:10.1029/2002JD002534
- 534 Gao, P., Geissen, V., Ritsema, C., Mu, X.-M., Wang, F., 2012. Impact of climate change and
535 anthropogenic activities on stream flow and sediment discharge in the Wei River basin, China. Hydrol.
536 Earth Syst. Sci. Discuss. 9, 3933–3959. doi:10.5194/hessd-9-3933-2012
- 537 [Grimaldi, S., 2004. Linear parametric models applied to daily hydrological series. J. Hydrol. Eng. 9, 383–](#)
538 [391. doi:10.1061/\(ASCE\)1084-0699\(2004\)9:5\(383\)](#)

Formatiert: Englisch (USA)

539 Huang, N.E., Shen, Z., Long, S.R., Wu, M.C., Shih, H.H., Zheng, Q., Yen, N.-C., Tung, C.C., Liu, H.H.,
540 1998. The empirical mode decomposition and the Hilbert spectrum for nonlinear and non-stationary time
541 series analysis. *Proc. R. Soc. London. Ser. A Math. Phys. Eng. Sci.* 454, 903–995.

542 Joe, H., 1997. *Multivariate models and multivariate dependence concepts*. Chapman&Hall, London.

543 Karlsson, I.B., Sonnenborg, T.O., Jensen, K.H., Refsgaard, J.C., 2014. Historical trends in precipitation
544 and stream discharge at the Skjern River catchment, Denmark. *Hydrol. Earth Syst. Sci.* 18, 595–610.
545 doi:10.5194/hess-18-595-2014

546 Lammersen, R., Engel, H., Van de Langemheen, W., Buiteveld, H., 2002. Impact of river training and
547 retention measures on flood peaks along the Rhine. *J. Hydrol.* 267, 115–124. doi:10.1016/S0022-
548 1694(02)00144-0

549 Li, J., 2010. *Application of copulas as a new geostatistical tool*. PhD Thesis. Nr. 187. University of
550 Stuttgart, Germany

551 Nelsen, R.B., 2006. *An Introduction to Copulas*. Springer, New York. doi:10.1007/0-387-28678-0

552 Pettitt, A.N., 1979. A non-parametric approach to the change-point problem. *Appl. Stat.* 126–135.

553 Samaniego, L., Bárdossy, A., Kumar, R., 2010. Streamflow prediction in ungauged catchments using
554 copula-based dissimilarity measures. *Water Resour. Res.* 46, W02506. doi:10.1029/2008WR007695

555 [Serfling, R., Xiao, P., 2007. A contribution to multivariate L-moments: L-comoment matrices. J. Multivar.
556 Anal. 98, 1765–1781. doi:10.1016/j.jmva.2007.01.008](#)

557 Sharifdoost, M., Mahmoodi, S., Pasha, E., 2009. A statistical test for time reversibility of stationary finite
558 state Markov chains. *Appl. Math. Sci.* 52, 2563–2574.

559 Siepe, A., 2006. *Dynamische Überflutungen am Oberrhein : Entwicklungs-Motor für die Auwald-Fauna.*
560 Stand 149–158.

561 Singh, S.K., McMillan, H., Bárdossy, A., 2013. Use of the data depth function to differentiate between
562 case of interpolation and extrapolation in hydrological model prediction. *J. Hydrol.* 477, 213–228.
563 doi:10.1016/j.jhydrol.2012.11.034

564 Sklar, A., 1959. *Fonctions de répartition à n dimensions et leurs marges*, Publications de l’Institut de
565 statistique de l’Université de Paris. Publications de l’Institut de Statistique de L’Université de Paris 8.

566 Sugimoto, T., 2014. *Copula based stochastic analysis of discharge time series*. PhD Thesis. Nr. 232.
567 University of Stuttgart, Germany

568 Wu, C.S., Yang, S.L., Lei, Y.P., 2012. Quantifying the anthropogenic and climatic impacts on water
569 discharge and sediment load in the Pearl River (Zhujiang), China (1954-2009). *J. Hydrol.* 452-453, 190–
570 204. doi:10.1016/j.jhydrol.2012.05.064

571

Formatiert: Englisch (USA)

Formatiert: Englisch (USA)

572

573 Table 1 Variance and copula variance calculated for 4 discharge time series

574
575

	ANDE	COCH	MAXA	PLOC
<i>Var</i>	1.79	2.24	1.75	2.72
<i>Var_{cop}</i> [$\times 10^{-5}$]	3.01	1.64	5.39	1.27

576

577 Table 2 Covariance, correlation, copula covariance and copula correlation between 4 discharge data

578 (AN:Andernach, CO:Cochem, MA:Maxau, PL:Plochingen)

579
580

	AN-CO	AN-MA	AN-PL	CO-MA	CO-PL	MA-PL
<i>Cov</i>	1.68	1.60	1.33	1.38	1.31	1.41
<i>Cor</i>	0.84	0.90	0.60	0.70	0.53	0.64
<i>Cov_{cop}</i> [$\times 10^{-6}$]	4.90	3.40	3.39	7.16	9.90	5.47
<i>Cor_{cop}</i>	0.60	0.77	0.46	0.71	0.60	0.59

581

582 Table 3 Variance and copula variance calculated for API time series of 4 regions in the Baden-

583 Württemberg state of Germany

584
585

	C	SW	NW	NE
<i>Var</i>	1.70	1.66	1.72	1.78
<i>Var_{cop}</i> [$\times 10^{-6}$]	3.00	4.02	3.35	3.21

586

587 Table 4 Covariance, correlation, copula covariance and copula correlation between API time series from 4
588 regions in the Baden-Württemberg state of Germany

589

590
591

	C-SW	C-NW	C-NE	SW-NW	SW-NE	NW-NE
<i>Cov</i>	1.35	1.33	1.44	1.25	1.41	1.42
<i>Cor</i>	0.80	0.77	0.84	0.74	0.84	0.83
<i>Cov_{cop}</i> [$\times 10^{-7}$]	1.46	1.16	8.94	4.42	1.11	8.80
<i>Cor_{cop}</i>	0.36	0.29	0.29	0.09	0.26	0.24

592

593 Figure Captions

594

595 Figure 1 Locations of 7 discharge gauging stations in the Upper Rhine Region

596 Figure 2 Visualization of the functions which displays the contribution of a realization of (U_t, U_{t+k}) to
597 *assymetry1* (left) and *assymetry2* (right)

598 Figure 3 Sketch of the transformation from sample hydrograph (left) to empirical copula (right):
599 Scatterplot of ranks are calculated from two values separated by time lag $k = 1$ [days] in a discharge time
600 series of Andernach where *rank correlation* = 0.9870, $A_1(k = 1) = -0.0002398$ and
601 $A_2(k = 1) = -0.00011037$. The possible combinations of high and low values, which has large impacts on
602 asymmetry, are numbered (1) low to high, (2) high to high (3) high to low (4) low to low. Negative
603 contribution to *assymetry2* is drawn with red circle, positive contribution with blue circle.

604 Figure 4 Annual cycle of mean discharge after smoothing (left) and annual cycle of standard deviation
605 after smoothing (right)

606 Figure 5 Discharge time series between 1950 and 1955 before applying normalization (upper left) and after
607 applying normalization (upper right). The variation of *assymetry2* function calculated for entire time
608 series before applying normalization (bottom left) and after applying normalization (bottom right) with
609 90% confidence intervals (grey) calculated for 100 realizations of Gaussian process (dashed line is $A_2(k)$
610 calculated for one of the realization of Gaussian process).

611 Figure 6 Relation between Asymmetry and catchment characteristics: minimum of *assymetry2* of
612 discharge and catchment area (top), lag at minimum of *assymetry2* of discharge and catchment area
613 (middle), minimum of *assymetry2* of discharge and lag at minimum of *assymetry2* of discharge (bottom)

614 Figure 7 Temporal change of minimum of *assymetry2* for 7 discharge records and confidence intervals
615 calculated from the Gaussian process (90% confidence interval with grey color and 60% confidence
616 interval with dark grey color) and one of its realizations (dashed line)

617 Figure 8 Moving average and standard deviation of the 7 daily discharge records for the window size $w =$
618 3000

619 Figure 9 Annual minimum and mean of aggregated daily temperature in the Baden-Württemberg state of
620 Germany

621 Figure 10 Copula distances of discharge time series in moving time window: moving variance (top),
622 distance type1 (middle) and distance type2 (bottom) with 80% confidence interval of Gaussian process and
623 one of its realization (dashed line)

624 Figure 11 Copula distances of discharge time series in moving time window: moving covariance (top),
625 moving correlation (second), distance type3 (third) and distance type4 (bottom)

626 Figure 12 Locations of the precipitation gauge stations within the Baden-Württemberg (Germany)
627 indicated by coloured circles. Upper Neckar catchment is drawn with green area and the location of
628 gauging station is drawn with a square

629 Figure 13 Copula distances of API time series in moving time window: moving variance (top), copula
630 distance type1 (middle) and copula distance type2 (bottom) where ‘C’ denotes central, ‘SW’ denotes
631 southwest, ‘NW’ denotes northwest and ‘NE’ denotes northeast part of Baden-Württemberg State of
632 Germany respectively with 80% confidence interval of Gaussian process and one of its realization (dashed
633 line).

634 Figure 14 Copula distances of API time series in moving time window: moving covariance (top), moving
635 correlation (second), distance type3 (third) and distance type4 (bottom)

636 Figure 15 Copula distance type3 (top) and type4 (bottom) between 4 discharge and 1 API time series
637 which is aggregated for all the daily precipitations depicted in Figure 12

638 Figure 16 Copula asymmetry and copula distances for 30 simulated and one observed discharge time series
639 at Plochingen between 1965 and 2000: minimum of asymmetry2 for the time lag $k = 2$ [days] (top), copula
640 distance type1 (middle), copula distance type2 (bottom)

641

642

643

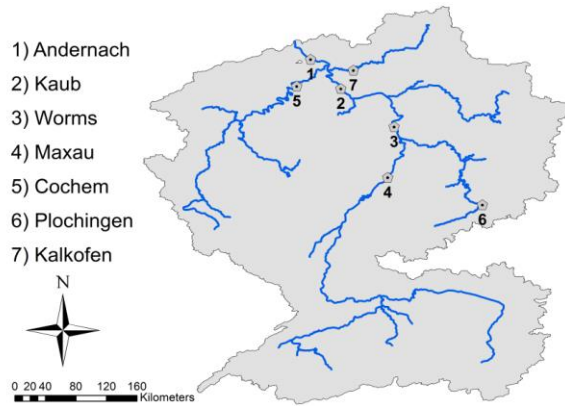


Figure 1 Locations of 7 discharge gauging stations in the Upper Rhine Region

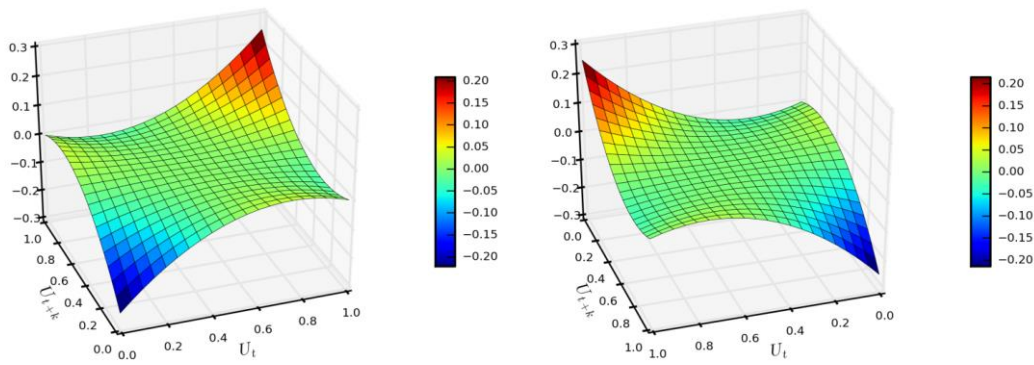
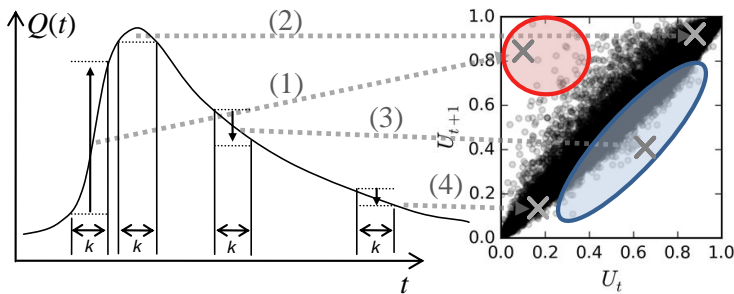


Figure 2 Visualization of the functions which displays the contribution of a realization of (U_t, U_{t+k}) to *assymetry1* (left) and *assymetry2* (right)



Formatiert: Zentriert

Figure 3 Sketch of the transformation from sample hydrograph (left) to empirical copula (right): Scatterplot of ranks are calculated from two values separated by time lag $k = 1$ [days] in a discharge time series of Andernach where rank correlation = 0.9870, $A_1(k = 1) = -0.0002398$ and $A_2(k = 1) = -0.00011037$. The possible combinations of high and low values, which has large impacts on asymmetry, are numbered (1) low to high, (2) high to high (3) high to low (4) low to low. Negative contribution to asymmetry2 is drawn with red circle, positive contribution with blue circle.

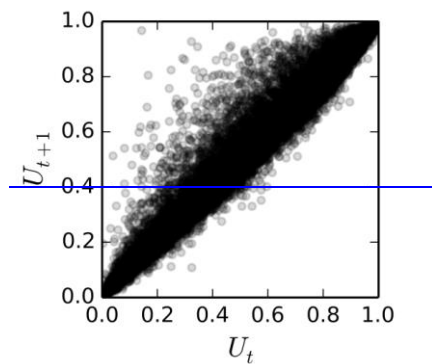


Figure 3 Scatterplot of ranks calculated from two values separated by time lag $k = 1$ [days] in a discharge time series of Andernach where rank correlation = 0.9870, $A_1(k = 1) = -0.0002398$ and $A_2(k = 1) = -0.00011037$

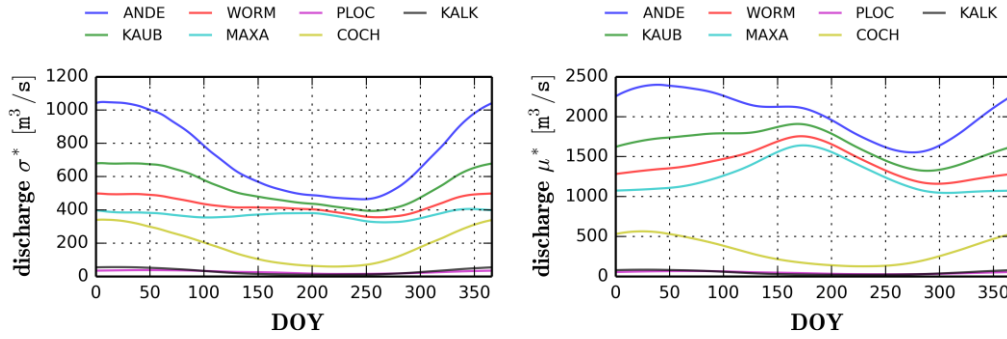


Figure 4 Annual cycle of mean discharge after smoothing (left) and annual cycle of standard deviation after smoothing (right)

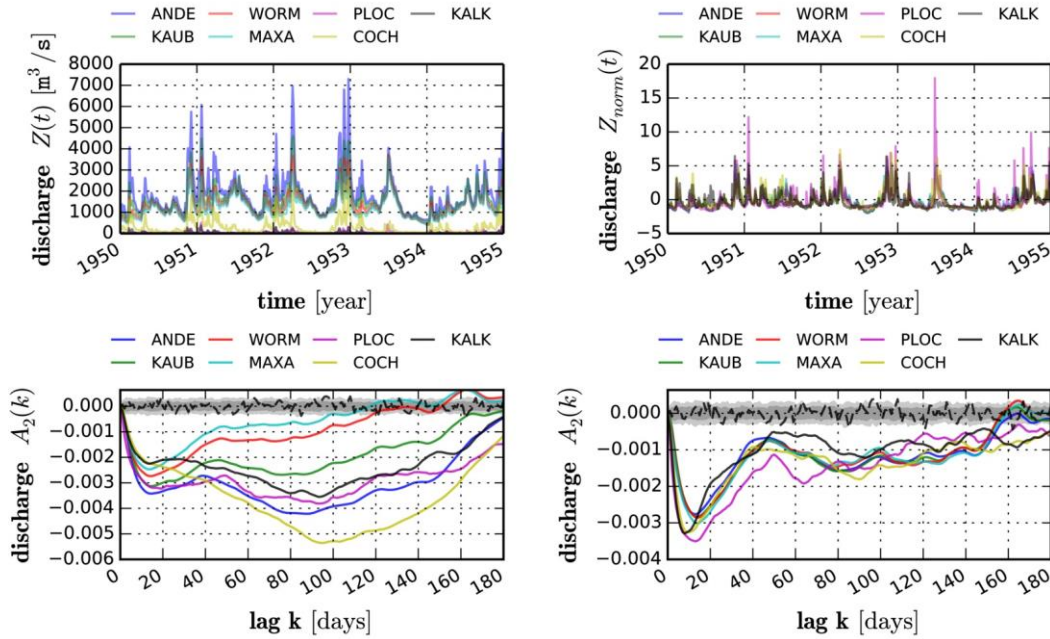
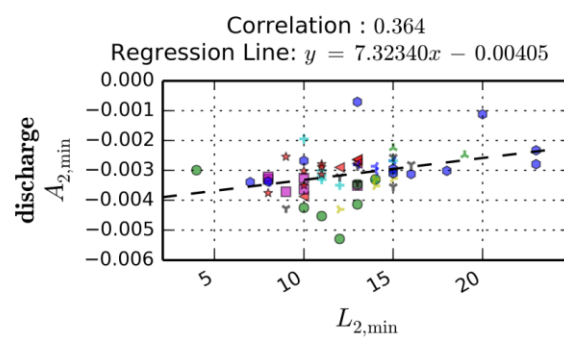
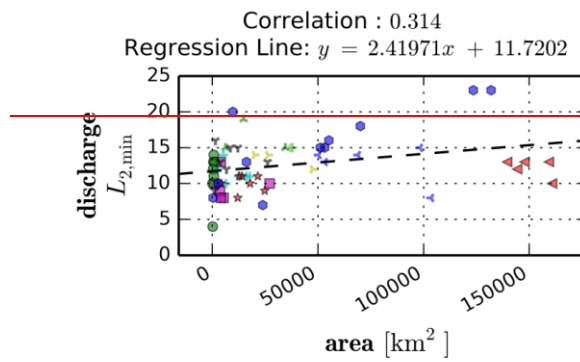
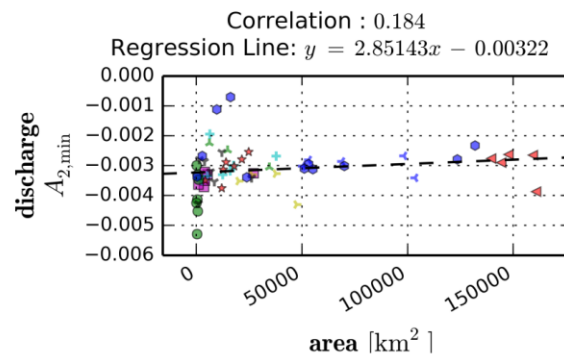
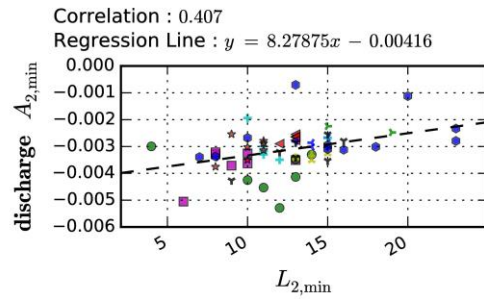
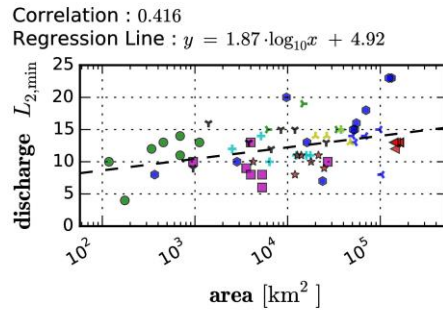
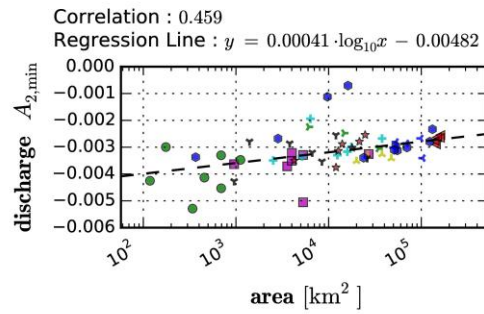


Figure 5 Discharge time series between 1950 and 1955 before applying normalization (upper left) and after applying normalization (upper right). The variation of asymmetry2 function calculated for entire time series before applying normalization (bottom left) and after applying normalization (bottom right) with 90% confidence intervals (grey) calculated for 100 realizations of Gaussian process (dashed line is $A_2(k)$ calculated for one of the realization of Gaussian process).

- ▲ Middle Rhine
 + Weser
 ▼ Danube (main stream)
- ▲ Upper Rhine
 ★ Main
 ▼ Danube (tributary)
- ▲ High Rhine
 ● Neckar
 ● Elbe
- Rhine (tributary)



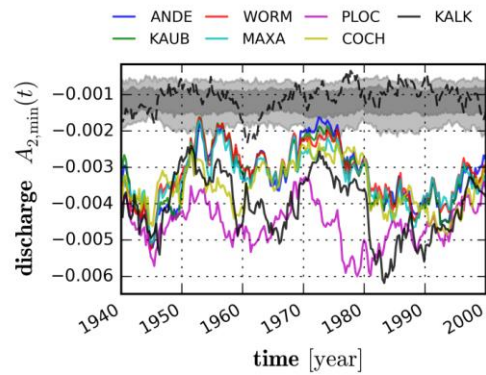
▲ Middle Rhine + Weser ▲ Danube (main stream)
 ▲ Upper Rhine ★ Main ▼ Danube (tributary)
 ▲ High Rhine ● Neckar ● Elbe
 ■ Rhine (tributary)



672

673 Figure 6 Relation between Asymmetry and catchment characteristics: minimum of asymmetry2 of
 674 discharge and catchment area (top), lag at minimum of asymmetry2 of discharge and catchment area
 675 (middle), minimum of asymmetry2 of discharge and lag at minimum of asymmetry2 of discharge (bottom)
 676

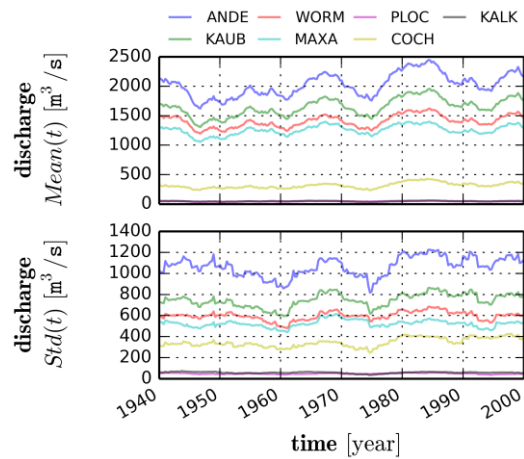
677



678

679 Figure 7 Temporal change of minimum of asymmetry2 for 7 discharge records and confidence intervals
680 calculated from the Gaussian process (90% confidence interval with grey color and 60% confidence
681 interval with dark grey color) and one of its realizations (dashed line)

682



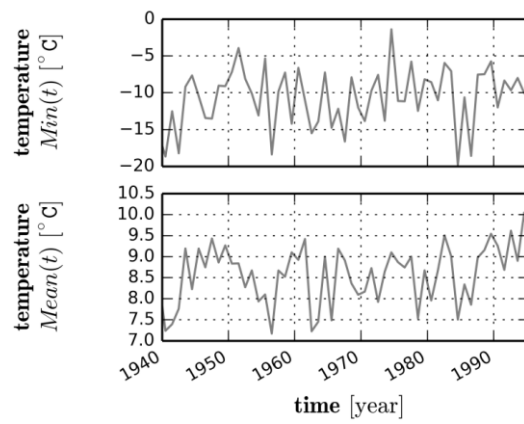
683

684 Figure 8 Moving average and standard deviation of the 7 daily discharge records for the window size $w =$
685 3000

686

687

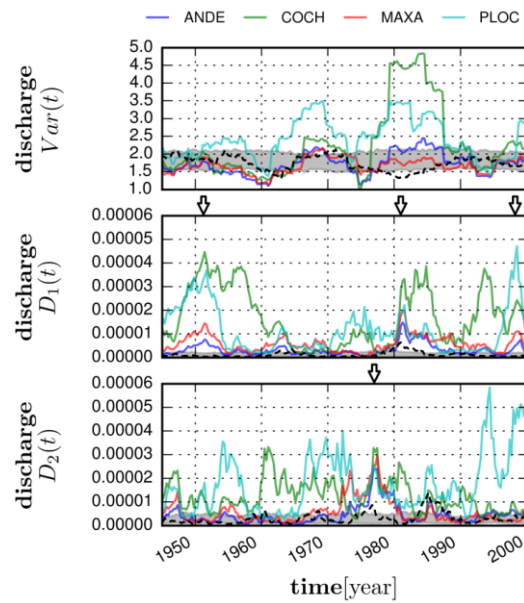
688



689

690 Figure 9 Annual minimum and mean of aggregated daily temperature in the Baden-Württemberg state of

691 Germany



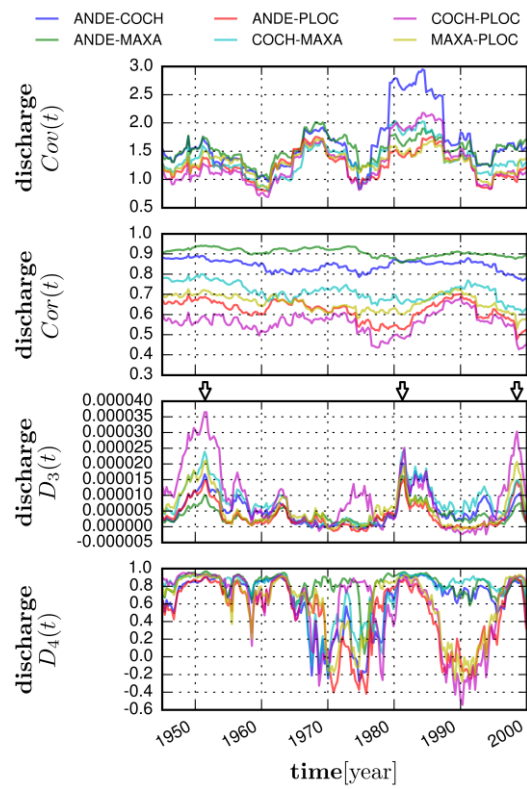
692

693 Figure 10 Copula distances of discharge time series in moving time window: moving variance (top),

694 distance type1 (middle) and distance type2 (bottom) with 80% confidence interval of Gaussian process and

695 one of its realization (dashed line)

696



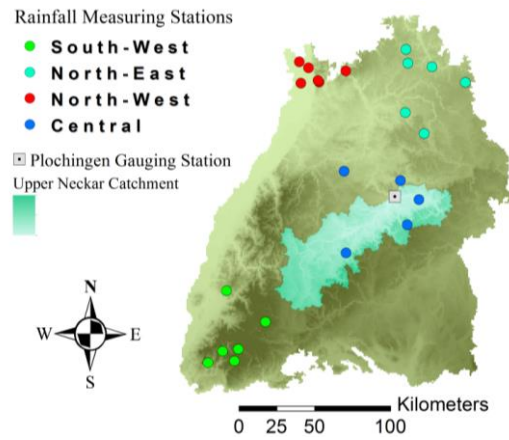
697

698 Figure 11 Copula distances of discharge time series in moving time window: moving covariance (top),

699 moving correlation (second), distance type3 (third) and distance type4 (bottom)

700

701



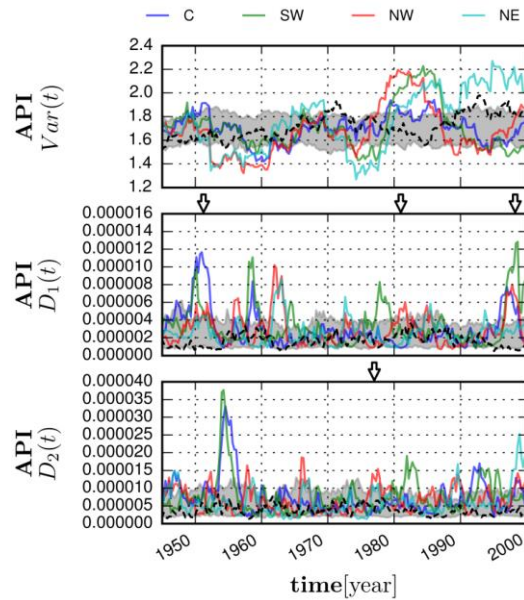
702

703 Figure 12 Locations of the precipitation gauge stations within the Baden-Württemberg (Germany)

704 indicated by coloured circles. Upper Neckar catchment is drawn with green area and the location of

705 gauging station is drawn with a square

706



707

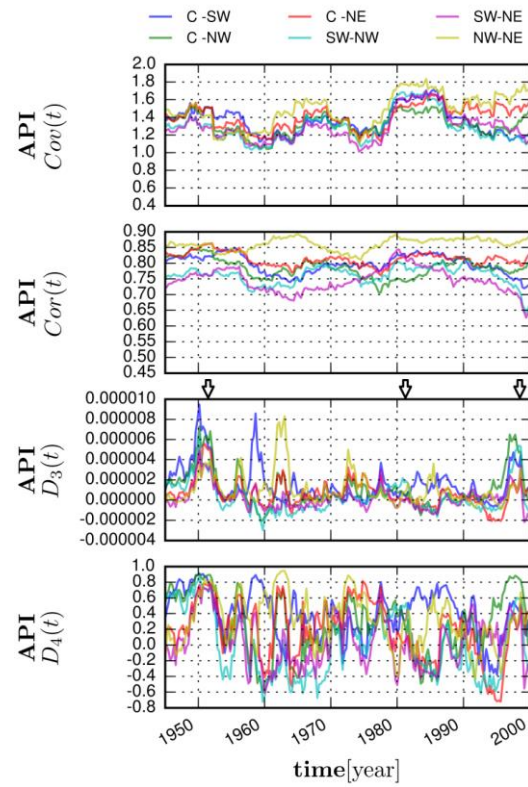
708 Figure 13 Copula distances of API time series in moving time window: moving variance (top), copula
709 distance type1 (middle) and copula distance type2 (bottom) where ‘C’ denotes central, ‘SW’ denotes
710 southwest, ‘NW’ denotes northwest and ‘NE’ denotes northeast part of Baden-Württemberg State of
711 Germany respectively with 80% confidence interval of Gaussian process and one of its realization (dashed
712 line).

713

714

715

716

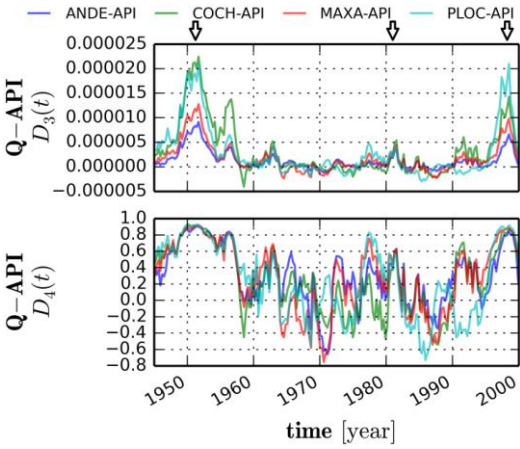


717

718 Figure 14 Copula distances of API time series in moving time window: moving
719 correlation (second), distance type3 (third) and distance type4 (bottom)

720

721

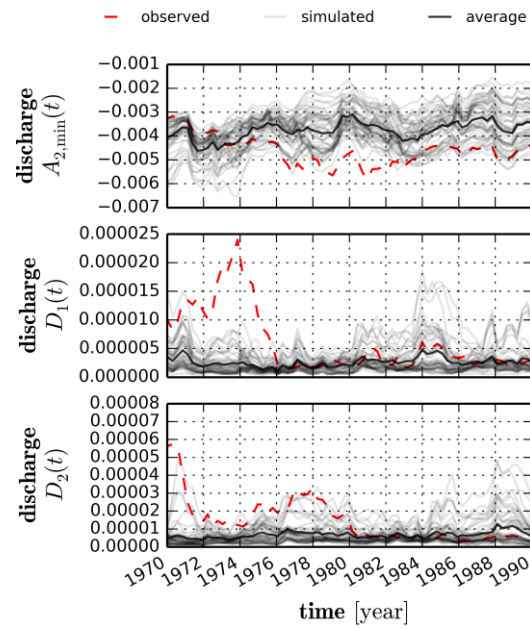


722

723 Figure 15 Copula distance type3 (top) and type4 (bottom) between 4 discharge and 1 API time series

724 which is aggregated for all the daily precipitations depicted in [Figure 12](#)~~Figure 12~~

725



726

727 Figure 16 Copula asymmetry and copula distances for 30 simulated and one observed discharge time series
728 at Plochingen between 1965 and 2000: minimum of asymmetry2 for the time lag $k = 2$ [days] (top), copula
729 distance type1 (middle), copula distance type2 (bottom)

730

731

732

733